Astronomy & Astrophysics manuscript no. hd
September 22, 2008

HD molecules at high redshift [⋆]

A low astration factor of deuterium in a solar-metallicity DLA system at $z = 2.418$

P. Noterdaeme[1], P. Petitjean[1], C. Ledoux[2], R. Srianand[3] and A. Ivanchik[4]

[1] Institut d'Astrophysique de Paris, CNRS - Université Pierre et Marie Curie, 98bis bd Arago, 75014 Paris, France
e-mail: `noterdaeme@iap.fr, petitjean@iap.fr`
[2] European Southern Observatory, Alonso de Córdova 3107, Casilla 19001, Vitacura, Santiago 19, Chile
e-mail: `cledoux@eso.org`
[3] Inter University Centre for Astronomy and Astrophysics, Post Bag 4, Ganesh Khind, Pune 411 007, India
e-mail: `anand@iucaa.ernet.in`
[4] Ioffe Physical Technical Institute, St Petersburg 194021, Russia
e-mail: `iav@astro.ioffe.ru`

Preprint online version: September 22, 2008

ABSTRACT

We present the detection of deuterated molecular hydrogen (HD) in the remote Universe in a damped Lyman-α cloud at $z_{\rm abs} = 2.418$ toward the quasar SDSS J143912.04+111740.5. This is a unique system in which H_2 and CO molecules are also detected. The chemical enrichment of this gas derived from Zn II and S II is as high as in the Sun. We measure $N({\rm HD})/2N({\rm H_2}) = 1.5^{+0.6}_{-0.4} \times 10^{-5}$, which is significantly higher than the same ratio measured in the Galaxy and close to the primordial D/H ratio estimated from the WMAP constraint on the baryonic matter density ($\Omega_{\rm b}$). This indicates a low astration factor of deuterium that contrasts with the unusually high chemical enrichment of the gas. This can be interpreted as the consequence of an intense infall of primordial gas onto the associated galaxy. Detection of HD molecules at high-z also opens the possibility to obtain an independent constraint on the cosmological-time variability of μ, the proton-to-electron mass ratio.

Key words. Cosmology: observations – Galaxies: high-redshift – Galaxies: ISM – Quasars: absorption lines – Quasars: individual: SDSS J143912.04+111740.5

1. Introduction

Deuterium is produced by primordial nucleosynthesis and is subsequently destroyed in stars. Therefore measurements of D/H from primordial gas provide important constraints on the baryonic matter density $\Omega_{\rm b}$ in the framework of Big-Bang cosmology (Wagoner, 1973). Measurements at different redshifts in turn provide important clues on the star formation history (Daigne et al., 2004; Steigman et al., 2007). All the available D/H measurements at high-z are based on the determination of the $N({\rm D^0})/N({\rm H^0})$ ratio in low-metallicity QSO absorption line systems. These measurements are difficult mainly because the velocity separation between D I and H I absorption lines is small ($\Delta v_{\rm D\,I/H\,I} \sim 80$ km s^{-1}) implying the lines are easily blended. An additional difficulty is the presence of the Lyman-α forest, making hard to find the true continuum position and to discern between D I absorption lines and intervening Ly-α forest lines. This explains why, despite more than a decade of efforts, only seven robust measurements of D/H at high-redshift have been performed (O'Meara et al., 2006; Pettini et al., 2008a). It happens that these measurements are consistent with the value $[{\rm D/H}]_{\rm p} = 2.55 \pm 0.10 \times 10^{-5}$ derived from the Wilkinson Microwave Anisotropy Probe (WMAP) five year data (Komatsu et al., 2008) together with the $\eta \leftrightarrow [{\rm D/H}]_{\rm p}$ conversion from Burles et al. (2001), where η is the baryon-to-photon ratio. We consider this $[{\rm D/H}]_{\rm p}$ value as the primordial D abundance in this work.

Damped Lyman-α systems (DLAs) are absorbers with the highest neutral hydrogen column densities among H I absorption line systems ($N({\rm H^0}) \gtrsim 10^{20}$ cm^{-2}) and are thought to arise from the neutral interstellar medium (ISM) of distant galaxies (Wolfe et al., 2005). Only a small fraction (∼10-15%) of them show detectable amounts of H_2 (Ledoux et al., 2003; Noterdaeme et al., 2008). Among the 14 high-z H_2-bearing DLAs known to date, only two show HD absorption (Varshalovich et al., 2001; Srianand et al., 2008). The $z_{\rm abs} = 2.418$ system toward SDSS J143912+111740 we present here is the only one where, in addition to H_2 and HD, CO is detected. From the excitation of CO it is possible to derive in a straightforward way an accurate estimate of the Cosmic Microwave Background Radiation temperature at the redshift of the absorber (Srianand et al., 2008). Here we focus on the HD/H_2 ratio and its implications for the star-formation history in the DLA galaxy.

2. Observations and Analysis

Observations were performed with the Ultraviolet and Visual Echelle Spectrograph of the Very Large Telescope at the European Southern Observatory on March 21-25, 2007 with total exposure time on source exceeding 8 h. Both blue and red spectroscopic arms were used simultaneously using dichroic settings with central wavelengths of resp. 390 nm and 580 nm (or 610 nm). The resulting wavelength coverage is 330−710 nm

---

[⋆] Based on observations carried out at the European Southern Observatory, under programme 278.A-5062 with the Ultraviolet and Visual Echelle Spectrograph installed at the Very Large Telescope, unit Kueyen, on mount Paranal in Chile.

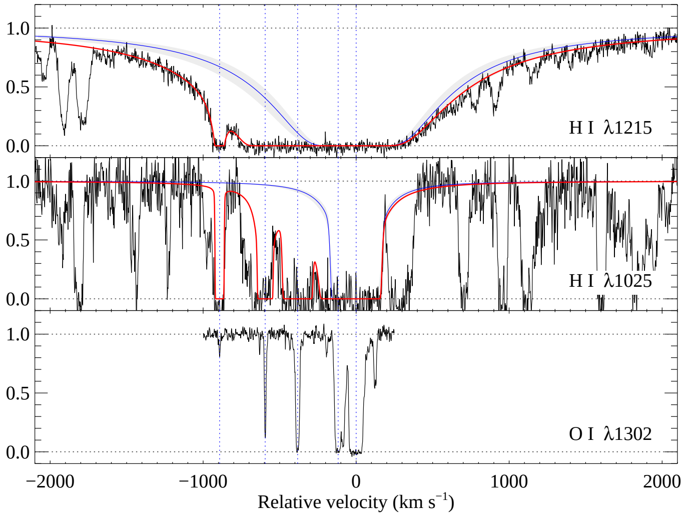

Fig. 1. Voigt profile fits to the Lyα (top panel) and Lyβ (middle panel) lines. The bottom panel shows the absorption profile of O I to visualize the positions of individual H I components (vertical dotted lines). The solid red lines indicate the overall fit-model. Profiles are plotted on a velocity scale with origin set at $z_{\rm abs}$ = 2.41837. Blue profiles at v = 0 km s^{-1} represent the main H^0 component and the associated uncertainty as a shaded region.

with a small gap between 452 and 478 nm. The CCD pixels were binned 2×2 and the slit width adjusted to 1″ matching the seeing conditions of ∼ 0.″9. This yields a resolving power of R = 50 000, as measured on the thorium-argon lines from the calibration lamp. The data were reduced using the UVES pipeline v 3.3.1 based on the ESO common pipeline library system. Accurate tracking of the object is achieved even in case of very low signal-to-noise ratio. Both the object and sky spectra are optimaly extracted and cosmic ray impacts and CCD defects are rejected iteratively. Wavelengths were rebinned to the vacuum-heliocentric rest frame and individual scientific exposures were co-added using a sliding window and weighting the signal by the total errors in each pixel. The dispersion around the wavelength calibration solution is 150 m s^{-1}. Standard Voigt-profile fitting methods were used for the analysis to determine column densities, redshifts, and Doppler parameters b.

H I absorption corresponding to the DLA is spread over ∼1000 km s^{-1}. The velocity structure can be modeled using the asymmetry of the Ly-α line and the profile of the Ly-β line (see Fig. 1). The derived structure is consistent with the velocity profile of the O I absorption. The latter species is believed to track H I closely through charge exchange reactions for $\log N({\rm H}^0) \geq 19.0$ (Viegas, 1995). The continuum is fitted at the same time as the absorption lines with a large-scale low-order spline.

The column density in the main clump is strongly constrained by the red damping wing and the gaps in the Ly-β absorption. The best fit gives $\log N({\rm H}^0) = 20.10^{+0.10}_{-0.08}$ for the main clump at $z_{\rm abs}$ = 2.41837. Note that a column density of $\log N({\rm H}^0) = 20.2$ would fill in the whole red profile (see Fig. 1). For a column density smaller than $\log N({\rm H}^0) = 20$, the shape of the profile can not be reproduced by any absorption located at −117 km s^{-1}.

The overall fit is represented in red on Fig. 1, while the contribution from the main clump only is shown by the blue profile and the associated uncertainties by the shaded region. Indicative column densities for other components are $\log N({\rm H}^0)$ = 17.9, 19.25, 19.20 and 19.20 at velocities v = −892, −594, −382, and −117 km s^{-1}, relative to the main clump studied here. The complex velocity structure and/or insufficient signal-to-noise ratio in the blue prevent the determination of $N({\rm D}^0)$ in these individual components directly from D I lines. From fitting together various optically thin transitions of S II, Zn II, Si II and Fe II, we derive metallicities in the main clump (at v = 0 km s^{-1}; see Table 1). No ionisation correction is applied. The presence of strong neutral carbon and molecular lines in the main clump, including easily photo-dissociated CO (Srianand et al., 2008) indicates that the effect of ionisation on abundances should be negligible. Indeed, in the abscence of neutral carbon, the ionisation correction for $\log N({\rm H\,I})$ = 20.1 is smaller than 0.10 dex (see Fig. 23 of Péroux et al., 2007). The S and Zn metallicities are solar and the relative depletion pattern (from Si and Fe) is typical of what is seen in cold neutral ISM clouds in the Galaxy (see Table 1).

Table 1. Observed metal abundances

Ion (X)	$\log N$(X)	[X/H][1]
S$^+$	15.27 ± 0.06	−0.03 ± 0.12
Zn$^+$	12.93 ± 0.04	+0.16 ± 0.11
Si$^+$	14.80 ± 0.04	−0.86 ± 0.11
Fe$^+$	14.28 ± 0.05	−1.32 ± 0.11
N^0	≥ 15.71	≥ −0.34

[1] with respect to solar abundances from Morton (2003).

3. Column densities of molecules and D/H ratio

Absorption lines from more than one hundred H$_2$ transitions from rotational levels J = 0 up to J = 5 are detected in the main H I component in six components spread over 50 km s^{-1}. Column densities in different J levels are obtained by simultaneous fits and are especially well constrained by the presence of damping wings seen on the corresponding lines from the Lyman 2-0, 4-0, 5-0, 7-0, 8-0, 9-0, and 10-0 bands and from the Werner 0-0 and 1-0 bands. Examples are shown on Fig. 2, with χ^2 = 1.04, 0.99 and 0.98 for J = 0, 1 and 3, respectively. We measure a total column density of $\log N({\rm H}_2) = 19.38 \pm 0.10$ and a molecular fraction, $f = 2N({\rm H}_2)/[2N({\rm H}_2)+N({\rm H}^0)] = 0.27^{+0.10}_{-0.08}$. The uncertainty on $N({\rm H}_2)$ is dominated by the error from fitting the damping wings of low rotational level lines (J = 0 and 1).

Deuterated molecular hydrogen is detected in the first rotational level in three components associated to the strongest H$_2$ components. Five HD absorption lines (L3-0 R0, L5-0 R0, L7-0 R0, L8-0 R0 and W0-0 R0) are clearly detected and were fitted simultaneously. The fits are shown on Fig. 2. Signal-to-noise ratios are ∼12 for L0-0 R0, L3-0 R0 and L5-0 R0, and ∼6 for the remaining lines. χ^2 values for the fit to these lines are 0.43 (L0-0 R0), 1.04 (L3-0 R0), 1.36 (L7-0 R0), 1.07 (L8-0 R0) and 1.49 (W0-0 R0). Note that fittings were done independently by two of us (PN and RS) with two different tools (FITLYMAN and VPFIT), yielding same results. The strongest constraint comes from L3-0 R0 transition which has good SNR and is optically thin (see Fig. 2). Note that L5-0 R0 is blended with another absorption and is not included in the fit. Results of the fits are summarized in Table 2. Errors correspond the fit of both the lines and the continuum. The total HD column density is $\log N({\rm HD}) = 14.87 \pm 0.025$.

Although each HD component is associated to one of the H$_2$ components, the strong blending of the latter, especially in low rotational levels, does not allow for the determination of

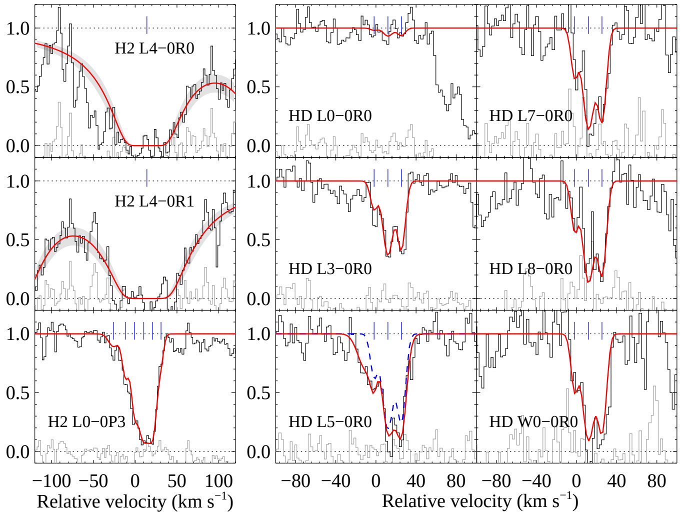

Fig. 2. Molecular hydrogen absorption lines. The normalized flux is given on a velocity scale with the origin set at $z_{\rm abs}$ = 2.41837. The Voigt profile fits as well as the residuals are also plotted. The blue dashed profile overplotted on HD L5-0 R0 corresponds to the contribution from HD only. The grey regions for H_2 L4-0 R0 and H_2 L4-0 R1 represent the 1σ uncertainty around the best fit. Short vertical lines mark the position of individual components.

Table 2. Voigt profile fitting results for HD

$z_{\rm abs}$	v^1 (km s^{-1})	b (km s^{-1})	log N(HD)
2.41835	−1.9	2.9 ± 0.8	13.89 ± 0.08
2.41851	12.0	5.0 ± 1.0	14.57 ± 0.04
2.41866	25.3	3.5 ± 0.3	14.46 ± 0.03

[1] Velocity relative to $z_{\rm abs}$ = 2.41837.

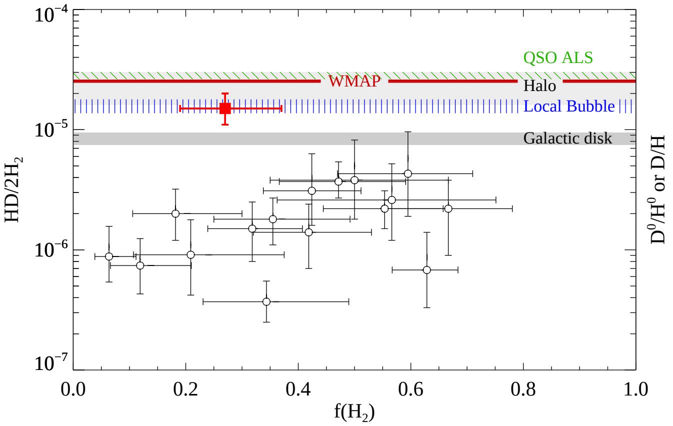

Fig. 3. The **HD/2H$_2$** ratio vs the molecular fraction. The filled square is the new measurement at $z_{\rm abs}$ = 2.418 toward SDSS J143912+111740. The empty circles are FUSE and Copernicus measurements in the Galactic ISM (Lacour et al., 2005). The grey region marks the D^0/H^0 ratio in the Galactic disk (Linsky et al., 2006), the light grey region marks this ratio in the Galactic halo (Savage et al., 2007) and the vertically-dashed one that in the Local Bubble (Moos et al., 2002; Linsky et al., 2006). The oblique dashed lines stand for D^0/H^0 measurements in high-redshift quasar absorption-line systems (QSO ALS; Pettini et al., 2008a). Finally, the solid line corresponds to the D/H ratio estimated from the baryon/photon ratio (WMAP; Komatsu et al., 2008).

N(HD)/2N(H_2) in individual components. We therefore use the column densities integrated over the whole profile for both HD and H_2 and obtain N(HD)/2N(H_2) = $1.5^{+0.6}_{-0.4}\times10^{-5}$. In Fig. 3, we compare the N(HD)/2N(H_2) ratio with similar measurements in the Galactic ISM (Lacour et al., 2005). It is apparent that the N(HD)/2N(H_2) ratio in the present system is an order of magnitude higher than the values for similar molecular fraction (and N(H_2)) measured in the Galaxy. We also compare these results to D^0/H^0 measurements in low metallicity clouds toward high-redshift quasars (Pettini et al., 2008a), the Galactic disk, the Galactic halo and the primordial D/H ratio estimated from the five-year WMAP results (Komatsu et al., 2008).

From the molecular ratio, HD/2H$_2$, we derive $({\rm D/H})_{DLA} > 0.7\times10^{-5}$ at the 95% confidence level. This corresponds to an astration factor $f_{\rm D} = ({\rm D/H})_{\rm p}/({\rm D/H})_{\rm DLA} < 3.6$ where $({\rm D/H})_{\rm p}$ refers to the primordial abundance derived from WMAP. However, the true (D/H) ratio (resp. astration factor) is probably well above the derived lower limit (resp. well below the upper limit) for various reasons:

First, the quoted HD/2H$_2$ ratio could represent a lower limit on the actual ratio in individual components as H_2 and HD are possibly not co-spatial. Indeed, the maximum HD column density does not arise in the strongest CO component (see Srianand et al., 2008), suggesting a fraction of the molecular hydrogen is not associated with HD.

Second, deriving the deuterium abundance from the HD column density is difficult because of the complex chemistry (e.g. Cazaux et al., 2008) and the sensitivity of the HD abundance on the particle density, cosmic ray density and UV field (Le Petit et al., 2002). However FUSE and Copernicus observations have shown that in the ISM of the Galaxy, the HD/H_2 ratio increases with the molecular fraction and that HD/2H$_2$ could trace D/H well only when $f \sim 1$ (Lacour et al., 2005), when both HD and H_2 are self-shielded from photo-dissociation. In diffuse gas, the HD optical depth is expected to be smaller than that of H_2 –as the deuterium abundance is low– and HD/2H$_2$ will provide a lower limit on D/H (Le Petit et al., 2002; Liszt, 2006). This is also supported by recent FUSE observations by Snow et al. (2008).

Finally, the D/H ratio in the gas phase, as measured by HD/2H$_2$, could itself be a lower limit on the true abundance ratio if depletion on dust is significant (Prochaska et al., 2005; Draine, 2006).

4. Discussion

Evidence for infall?

The high D/H ratio inferred above indicates that astration of deuterium is low eventhough metallicity is solar. This situation is well explained in our Galaxy by models including infall of primordial material (Steigman et al., 2007; Romano et al., 2006; Prodanović & Fields, 2008).

If we use the sulfur abundance as a proxy for that of oxygen, we note that the [N/O] ratio in the main H I component is consistent with the ratio expected for secondary nitrogen production at solar metallicity (Centurión et al., 2003; Petitjean et al., 2008; Pettini et al., 2008b). In addition, the [S/Zn] ratio is consistent with the solar value and does not indicate any α-enhancement.

The inferred lower limit on D/H, the near solar value of [α/Fe] and [N/α] rule out rapid star formation that is generally invoked to explain high chemical enrichment in elliptical galaxies.

Speculating slightly further, we note that the metal profile is spread over at least 800 $\mathrm{km\,s^{-1}}$ (see Fig. 1). This, together with the solar metallicity, is consistent with the gas being associated with a deep potential well (Ledoux et al., 2006).

The properties of the gas in the present system are similar to those of the ISM in our Galaxy. But these properties are reached on a time-scale five times smaller for the DLA galaxy than for the Milky Way, as the age of the Universe at $z = 2.42$ is 20% of its present age adopting the most recent cosmological parameters (Komatsu et al., 2008). This must imply that the system has undergone continuous star-formation and infall.

If one assumes negligible production of deuterium by cosmic rays and that this element is completely destroyed in the material that goes through stars then the gas infall rate $\dot{\mathrm{M}}_{\mathrm{in}}$ should on average be of the order of the star formation rate $\dot{\mathrm{M}}_{\mathrm{SFR}}$ in order to replenish deuterium. Recently several observational evidences have been published for cold gas accretion onto massive galaxies at high-z (Weidinger et al., 2005; Nilsson et al., 2006; Dijkstra et al., 2006) and low-z (Fraternali & Binney, 2008). In addition, numerical simulations suggest that at $z = 2 - 3$ the accretion of cold material from the IGM dominates for halos with masses $<\sim 3 \times 10^{11}$ $\mathrm{M}_\odot$ (Kereš et al., 2005). Interestingly, the inference that $\dot{\mathrm{M}}_{\mathrm{in}} \sim \dot{\mathrm{M}}_{\mathrm{SFR}}$ is also required to understand the properties of $z = 2 - 3$ Lyman-break galaxies (Erb, 2008). Our observations reinforce this important finding.

Constraint on the variability of μ

The detection of several HD transitions should make it possible to test the time variation of $\mu = m_p/m_e$, the proton-to-electron mass ratio. H_2 transitions at high redshift have been used (e.g., Ivanchik et al., 2005; Reinhold et al., 2006; King et al., 2008) to probe the variability of μ. This is done by measuring the relative position of the lines around the overall redshift of the absorbing cloud,

$$\zeta_i = (z_i - \overline{z}_{\mathrm{abs}})/(1 + \overline{z}_{\mathrm{abs}}) = \frac{\Delta\mu}{\mu} K_i \ ,$$

where $z_i = \lambda_i/\lambda_i^0 - 1$ is the observed redshift of line i and $K_i = d\ln\lambda_i^0/d\ln\mu$ is the sensitivity on μ calculated for each transition. $\overline{z}_{\mathrm{abs}}$ is taken for each component as the weighted mean redshift from the different transitions. As these measurements may involve various unknown systematics, it is important to use different sets of lines and different techniques. Sensitivity coefficients and accurate wavelengths for HD transitions have been published very recently (Ivanov et al., 2008). However, the SNR of our data at the position of the HD absorption lines prevents us to perform a measurement at the level of current studies. Additional data on this quasar are needed to be able to derive an independent constraint on the variability of μ.

5. Conclusion

We reported the detection of HD molecules at $z_{\mathrm{abs}} = 2.418$ toward SDSS J143912+111740, following a careful selection of quasars in the SDSS database and intensive observations with UVES at the Very Large Telescope. The system presents characteristics very similar to what is observed in the solar neighbourhood. We find $\mathrm{HD}/2\mathrm{H}_2 = 1.5 \times 10^{-5}$, consistent with an astration factor of deuterium less than 1.7 which is contrasting with the high chemical enrichment. This is best explained by a scenario in which the gas that goes through star formation is replenished by continuous infall of ambient primordial gas. Similar results arise from recent numerical simulations and semi-analytical models (e.g. Kereš et al., 2005; Erb, 2008). Interestingly, dynamical studies of nearby galaxies (Fraternali & Binney, 2008) as well as interpretation of Ly-α blobs at high redshift (Weidinger et al., 2005; Nilsson et al., 2006; Dijkstra et al., 2006) provide independent observational evidences for accretion of gas onto massive galaxies.

We finally stress the importance of detecting similar systems to probe the time-variation of the proton-to-electron mass ratio from HD lines. Although such a independent test would be welcome to characterize possible unknown systematics, significantly higher signal-to-noise ratio is required to obtain limits comparable to those obtained with other techniques.

Acknowledgements. We thank an anonymous referee for comments and suggestions that improved the quality of the paper. We warmly thank the ESO Director Discretionary Time allocation committee and the ESO Director General, Catherine Cesarsky, for allowing us to carry out these observations. PPJ and RS gratefully acknowledge support from the Indo-French Centre for the Promotion of Advanced Research (Centre Franco-Indien pour la Promotion de la Recherche Avancée).

References

Burles, S., Nollett, K. M., & Turner, M. S. 2001, ApJ, 552, L1
Cazaux, S., Caselli, P., Cobut, V., & Le Bourlot, J. 2008, A&A, 483, 495
Centurión, M., Molaro, P., Vladilo, G., et al. 2003, A&A, 403, 55
Daigne, F., Olive, K. A., Vangioni-Flam, E., Silk, J., & Audouze, J. 2004, ApJ, 617, 693
Dijkstra, M., Haiman, Z., & Spaans, M. 2006, ApJ, 649, 37
Draine, B. T. 2006, in Astronomical Society of the Pacific Conference Series, Vol. 348, Astrophysics in the Far Ultraviolet: Five Years of Discovery with FUSE, ed. G. Sonneborn, H. W. Moos, & B.-G. Andersson, 58–+
Erb, D. K. 2008, ApJ, 674, 151
Fraternali, F. & Binney, J. J. 2008, MNRAS, 375
Ivanchik, A., Petitjean, P., Varshalovich, D., et al. 2005, A&A, 440, 45
Ivanov, T. I., Roudjane, M., Vieitez, M. O., et al. 2008, Phys. Rev. Lett., 100, 093007
Kereš, D., Katz, N., Weinberg, D. H., & Davé, R. 2005, MNRAS, 363, 2
King, J. A., Webb, J. K., Murphy, M. T., & Carswell, R. F. 2008, ArXiv e-prints, 807
Komatsu, E., Dunkley, J., Nolta, M. R., et al. 2008, ArXiv e-prints, 803
Lacour, S., André, M. K., Sonnentrucker, P., et al. 2005, A&A, 430, 967
Le Petit, F., Roueff, E., & Le Bourlot, J. 2002, A&A, 390, 369
Ledoux, C., Petitjean, P., Fynbo, J. P. U., Møller, P., & Srianand, R. 2006, A&A, 457, 71
Ledoux, C., Petitjean, P., & Srianand, R. 2003, MNRAS, 346, 209
Linsky, J. L., Draine, B. T., Moos, H. W., et al. 2006, ApJ, 647, 1106
Liszt, H. S. 2006, A&A, 452, 269
Moos, H. W., Sembach, K. R., Vidal-Madjar, A., et al. 2002, ApJS, 140, 3
Morton, D. C. 2003, ApJS, 149, 205
Nilsson, K. K., Fynbo, J. P. U., Møller, P., Sommer-Larsen, J., & Ledoux, C. 2006, A&A, 452, L23
Noterdaeme, P., Ledoux, C., Petitjean, P., & Srianand, R. 2008, A&A, 481, 327
O'Meara, J. M., Burles, S., Prochaska, J. X., et al. 2006, ApJ, 649, L61
Péroux, C., Dessauges-Zavadsky, M., D'Odorico, S., Kim, T.-S., & McMahon, R. G. 2007, MNRAS, 382, 177
Petitjean, P., Ledoux, C., & Srianand, R. 2008, A&A, 480, 349
Pettini, M., Zych, B. J., Murphy, M. T., Lewis, A., & Steidel, C. C. 2008a, ArXiv e-prints, 805
Pettini, M., Zych, B. J., Steidel, C. C., & Chaffee, F. H. 2008b, MNRAS, 385, 2011
Prochaska, J. X., Tripp, T. M., & Howk, J. C. 2005, ApJ, 620, L39
Prodanović, T. & Fields, B. D. 2008, Journal of Cosmology and Astro-Particle Physics, 9, 3
Reinhold, E., Buning, R., Hollenstein, U., et al. 2006, Phys. Rev. Lett., 96, 151101
Romano, D., Tosi, M., Chiappini, C., & Matteucci, F. 2006, MNRAS, 369, 295
Savage, B. D., Lehner, N., Fox, A., Wakker, B., & Sembach, K. 2007, ApJ, 659, 1222
Snow, T. P., Ross, T. L., Destree, J. D., et al. 2008, ArXiv e-prints, 808

Srianand, R., Noterdaeme, P., Ledoux, C., & Petitjean, P. 2008, A&A, 482, L39
Steigman, G., Romano, D., & Tosi, M. 2007, MNRAS, 378, 576
Varshalovich, D. A., Ivanchik, A. V., Petitjean, P., Srianand, R., & Ledoux, C. 2001, Astron. Letters, 27, 683
Viegas, S. M. 1995, MNRAS, 276, 268
Wagoner, R. V. 1973, ApJ, 179, 343
Weidinger, M., Møller, P., Fynbo, J. P. U., & Thomsen, B. 2005, A&A, 436, 825
Wolfe, A. M., Gawiser, E., & Prochaska, J. X. 2005, ARA&A, 43, 861